

Enhanced emission of a pyridine-based luminogen by hydrogen-bonding to organic and polymeric phenols†

Wei-Lun Chien, Chih-Min Yang, Tai-Lin Chen, Shu-Ting Li and Jin-Long Hong*

Cite this: *RSC Advances*, 2013, 3, 6930

Fluorescent bis(pyridinylvinyl)anthracene (An2Py) with two pyridine terminals was synthesized and used to prepare miscible blends with hydroxyl-containing components (organic bisphenol A (BPA) and polymeric poly(vinyl phenol) (PVPh)) through the facile intermolecular hydrogen-bond (H-bond) interactions between the pyridine and the hydroxyl functions. Before blending, the solution of An2Py already emits appreciably due to its aggregation-induced emission enhancement (AIEE) behavior; after blending with the hydroxyl components, the fluorescence can be further intensified due to the restricted molecular rotation, which leads to the blockage of non-radiative decay channels, imposed by the H-bond interactions. The role of the H-bonding on the restricted molecular rotation of the An2Py/BPA (and the An2Py/PVPh) blends was characterized by solution ^1H NMR and solid infrared spectroscopy. The effectiveness of the organic BPA and the polymeric PVP as molecular anchors to lock the free rotation of the An2Py luminogen were compared and discussed in this study.

Received 19th September 2012,
Accepted 25th February 2013

DOI: 10.1039/c3ra22217a

www.rsc.org/advances

Introduction

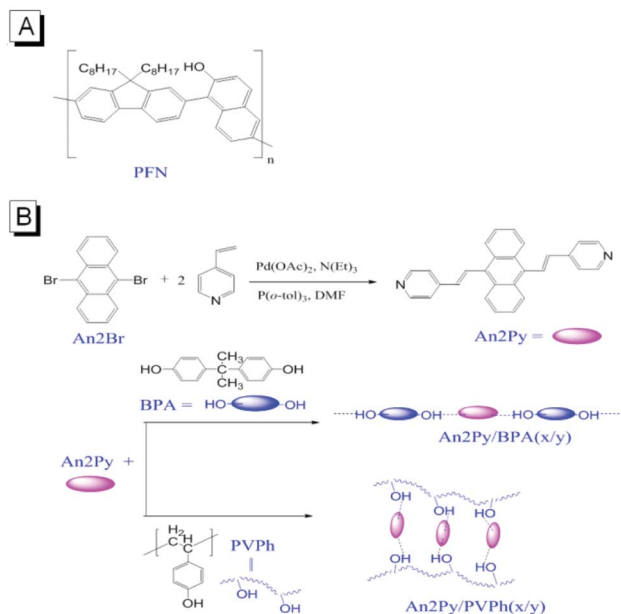
In 2001, Tang's group^{1,2} found that the non-coplanar 1-methyl-1,2,3,4,5-pentaphenylsilole (MPS) luminogen has interesting fluorescence behavior where it emits strongly when aggregated in solution and in the solid film state, despite its non-emissive character in the dilute solution state. In contrast to the aggregation-caused quenching (ACQ) observed in planar organic luminogens, this enhanced emission in the aggregated state had been designated as aggregation-induced emission (AIE). With beneficial emission efficiency in the film state, lots of organic and polymeric luminogens with AIE or AIE enhancement (AIEE) properties^{3–31} have been prepared and studied in order to improve fluorescent emission efficiency and to understand the operative mechanism leading to the observed enhanced emissions. Among several possibilities, restricted intramolecular rotation^{32,33} had been previously identified to be the main mechanism responsible for the observed AIE or AIEE behavior of silole compounds. In the aggregated states of silole compounds, the restricted molecular rotation of the phenyl groups reduces the possibilities of non-radiative decay pathways and results in the enhanced emission.

Physical forces, such as hydrogen-bond (H-bond) interactions, can be used to restrict the molecular rotation of organic luminogens. A fluorenone-derivative of 2,7-bis(4-(*tert*-

butylthio)phenyl)-fluorenone (DSFO)³⁴ was reported to have enhanced excimer emissions due to intermolecular H-bonds. The dimer structure of DSFO was locked by intermolecular H-bonds and the corresponding excimer emission therefore underwent fewer non-radiative decay pathways. The salicylideneaniline (SA)³⁵ compound forms a gel in certain organic solvents. The gel solution emits strongly with a fluorescent quantum yield (Φ_F) 600 times higher than that of the homogeneous solution. The AIEE property is ascribed to the formation of *J*-aggregates and the inhibition of molecular rotation by H-bond interactions. Other compounds containing hydrazine³⁶, benzoxazole³⁷, acrylamido³⁸ and naphthalide³⁹ functions were also found to exhibit enhanced emission in the gels, promoted by H-bond interactions. A polymeric system of poly(fluorene-*alt*-naphthol)⁴⁰ (PFN, Scheme 1A) prepared in our laboratory was also found to exhibit AIEE properties due to the restricted molecular rotation promoted by inter and intrachain H-bonds among the inherent hydroxyl groups. The restricted molecular rotation of PFN can be further enhanced by blending it with different amounts of poly(*N*-vinyl pyrrolidone)⁴¹ (PVR). Through the facile intermolecular H-bond interactions between PFN and PVR, a PFN/PVR blend with small amounts (2.3 wt%) of PFN can emit with a high Φ_F value of 93%. Use of H-bond interactions to lock the molecular rotations of organic and polymeric luminogens was therefore illustrated by the above examples. With effective restriction on molecular rotation, AIEE-active luminogens possess a beneficial strong emission in aggregated solution and in the solid state, which facilitates their solid-state applications (*e.g.* as a light-emitting layer in an organic light-emitting diode (OLED)). Under the premise that the emission performance can be

Department of Materials and Optoelectrical Science, National Sun Yat-Sen University, Kaohsiung, 80424, Taiwan. E-mail: jlhong@mail.nsysu.edu.tw;
Tel: +886 07 5252000 ext. 4065

† Electronic supplementary information (ESI) available: Fig. S1–S5. See DOI: 10.1039/c3ra22217a



Scheme 1 (A) Structure of PFN and (B) synthesis of An2Py and its mixing with BPA and PVPh to form An2Py/BPA(*x/y*) and An2Py/PVPh(*x/y*) blends, respectively.

maintained or enhanced, blending the valuable AIEE-active luminogens with other inexpensive, commercialized materials provides alternative routes to cut down the costs in practical applications. Because the H-bond interaction can effectively hinder the molecular rotation of non-coplanar AIEE-active fluorophores, blending AIEE-active luminogens with other H-bond interaction pairs was therefore attempted in this study. Here, the AIEE-active luminogen of bis(pyridinylvinyl)anthracene (An2Py in Scheme 1B) was used as a H-bond acceptor to react with H-bond donors of small-mass bisphenol A (BPA) and polymeric poly(vinyl phenol) (PVPh). Distinct from the above-mentioned PFN/PVR⁴¹ system, the use of small-mass An2Py here was based on its higher molecular mobility to produce more H-bond pairs compared to the polymeric PFN. The preferential H-bond interaction of the pyridine ring with the hydroxyl group of BPA (and PVPh) should operate to inhibit molecular rotation and further enhance fluorescence of the AIEE-active An2Py luminogen. With respect to molecular mobility and chain viscosity, the small-mass BPA and the polymeric PVPh are supposed to have different extents of restriction forces on the molecular rotation of the An2Py and therefore were used to form two blend systems for comparison. The correlations of H-bond interaction to restricted molecular rotation and to the emission efficiency are characterized through the application of ¹H NMR, infrared and emission spectroscopies and the results are summarized in this study.

Experimental section

Materials

Reagent grade anthracene, chloroform (CHCl₃), Br₂, tri-*o*-tolylphosphine, 4-vinylpyridine, poly(vinyl phenol) (*M_w* ~ 22 000) and dichloromethane (DCM) were purchased from Aldrich Chemical Co. and used directly without purification. *N,N*-Dimethylformamide (DMF) and Pd(OAc)₂ was purchased from Echo chemical Co. and DMF was refluxed over CaH₂ under nitrogen for 5 h before distillation for use.

Synthesis of 9,10-dibromoanthracene (An2Br)

Synthesis of An2Br was performed according to the reported procedures⁴² but with minor modification on purification step: To a solution of 5.0 g (28.05 mmol) anthracene in CHCl₃ (100 mL), two eq. Br₂ (2.9 mL, 56.1 mmol) in 50 mL of CHCl₃ was dropped slowly in the dark. After stirring for an additional 4 h the whole reaction mixture was poured into methanol (500 mL) to removed excess Br₂ and the crude reaction product was recrystallized from CH₂Cl₂ to yield the product as yellow needles; Yield: 9.05 g (96%); ¹H-NMR (500 MHz, chloroform-*d*): δ 8.62–8.56 (m, 4H, Ar-H), 7.66–7.61 (m, 4H, Ar-H) (Fig. S3, ESI†); MS *m/z*: found, 336.2. Anal. calcd for C₁₄H₈Br₂: C, 49.69; H, 2.26. Found: C, 49.75; H, 2.20.

Synthesis of bis(pyridinylvinyl)anthracene (An2Py)

A reaction mixture of 4-vinylpyridine (3.3 mL, 29.77 mmol), An2Br (5 g, 14.89 mmol), triethylamine (4 mL), Pd(OAc)₂ (0.33 g, 1.47 mmol) and tri-*o*-tolylphosphine (0.22 g, 0.72 mmol) in dry DMF (100 mL) was placed in a predried round-bottomed flask (250 mL). The reaction mixture was then degassed by freeze–pump–thaw 3 times before being heated at 110 °C for 24 h. After cooling to room temperature, the reaction mixtures were poured into water and the resultant suspensions were extracted with CH₂Cl₂ (3 × 40 mL). The combined organic extracts were washed with brine, dried over MgSO₄ and concentrated by rotary evaporator. The crude product was then purified by flash column chromatography (v/v hexane/ethyl acetate = 4/1) to give 1.51 g yellow An2Py as the final product. Yield: 1.51 g (26%); ¹H NMR (500 MHz, THF-*d*₈): δ 6.57–6.66 (d, 2H, –C=CH, *J*_{trans} = 16.5 Hz), 7.12–7.49 (m, 8H, Ar-H), 7.92–8.02 (d, 2H, –C=CH, *J*_{trans} = 16.5 Hz), 8.05–8.11 (m, 4H, Ar-H), 8.31–8.45 (d, 4H, Ar-H) (Fig. S4, ESI†); MS *m/z*: found, 384.3; Anal. calcd for C₂₈H₂₀N₂: C, 87.47; H, 5.24; N, 7.29. Found: C, 87.57; H, 5.19; N, 7.24.

Instrumentation

¹H NMR spectra were recorded with a Varian Unity Inova-500 MHz FT-NMR instrument. Tetramethylsilane (TMS) was used as the internal standard. The molar masses of the organic molecules were determined by a Bruker Autoflex III MALDI/TOF mass spectrometer. PL emission spectra were obtained from a LabGuide X350 fluorescence spectrophotometer using a 450 W Xe lamp as the continuous light source. UV-vis absorption spectra were recorded with an Ocean Optics DT1000 CE 376 spectrophotometer. A quartz cell with dimensions of 0.2 × 1.0 × 4.5 cm³ was used for the UV-Vis absorption and PL emission spectra measurements. Stock solutions of the organic and polymeric fluorophores with a

concentration of 10^{-4} M in THF were first prepared. Aliquots of these stock solutions were transferred to 10 mL volumetric flasks, into which appropriate volumes of THF and hexane were added dropwise under vigorous stirring to furnish 10^{-5} M solutions with different hexane contents (0–90 vol%). UV-Vis and PL emission spectroscopy were immediately performed once the solutions were prepared. Solid samples were prepared by drop-casting sample solutions over quartz plates. Fluorescence quantum yields (Φ_F) of the solution mixtures with varied compositions were determined by comparison with a quinine sulfate standard ($\Phi_F = 54\%$ in 0.05 M H_2SO_4). An integrating sphere was used for the film sample. FT-IR spectra were obtained on a Nicolet IR-200 spectrometer. Sample solution was dropped on a KBr pellet and dried under vacuum to prepare the solid film for FT-IR analysis. The wide-angle X-ray (WAXR) diffraction pattern of the solid blend was obtained from a Siemens D5000 diffractometer. Particle sizes of the aggregates in solution were measured by dynamic light scattering (DLS) using a Brookhaven 90 plus spectrometer equipped with a temperature controller. An argon ion laser operating at 658 nm was used as the light source.

Results and discussion

As illustrated in Scheme 1B, the An2Py luminogen can be readily prepared from the corresponding Heck-coupling reaction between 9,10-dibromoanthracene and 4-vinylpyridine. The two pyridine terminal rings of An2Py can be H-bonded to the hydroxyl groups of BPA and PVPh to form An2Py/BPA(x/y) and An2Py/PVPh(x/y) (x/y : refer to the molar ratio between the pyridine and the hydroxyl functions) blends, respectively. Except for the terminal rings (pyridine vs. benzene), the chemical structure of An2Py is similar to the reported AIEE-active 9,10-bis(*E*)-2-phenylanthracene⁴³ luminogen; therefore, An2Py is expected to have enhanced emission in the aggregated state and is characterized beforehand.

AIEE properties of An2Py

The AIEE property of An2Py was primarily evaluated by its PL emission spectra in THF/hexane solvent/poor solvent mixtures (Fig. 1A). Despite the high dilution (10^{-6} M) in pure THF solvent, the An2Py luminogen already emits with appreciable intensity and the solution fluorescence can be further intensified with increasing hexane content (while keeping the concentration of An2Py at 10^{-6} M) to generate aggregates in the solution mixtures. Formation of aggregated particles in the solution mixtures can be confirmed from the DLS analysis. The results summarized in Fig. 1B suggest that aggregated particles with an average hydrodynamic diameter (D_h) between 185 to 125 nm are resolved in the solution mixtures. With increasing hexane content in the solution mixtures, the resultant aggregated particles reduced their sizes and An2Py molecules in THF/hexane (v/v) = 1/9 solution form nanoparticles with the smallest size (with $D_h \sim 125$ nm) among all three solutions. Suggestively, free rotation of An2Py luminogen is supposed to be restricted within the confined spaces of the

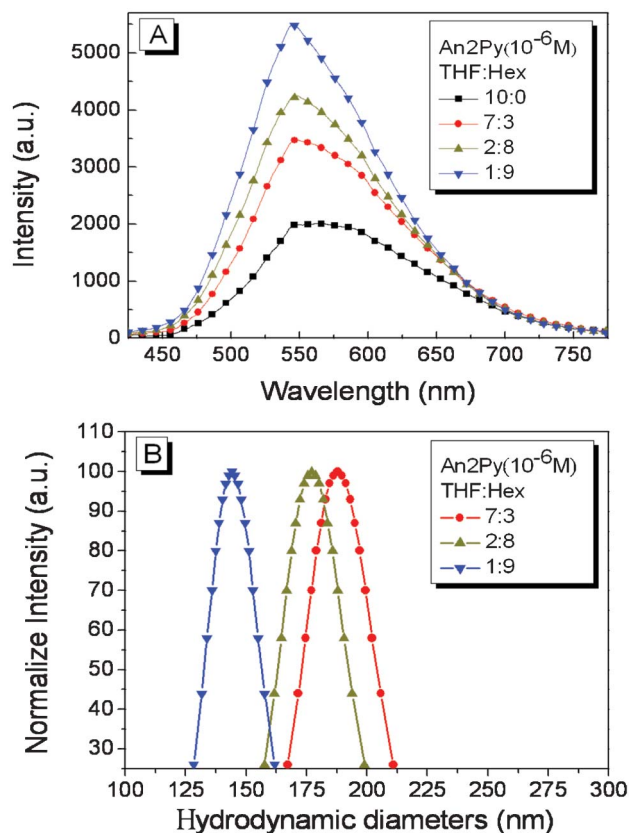


Fig. 1 (A) The PL emission spectra (excited at 400 nm) and (B) the hydrodynamic diameters of An2Py (10^{-6} M) in THF/hexane solvent mixtures of different volumetric (v/v) ratios.

aggregated particles due to the steric constraints imposed by the congested environment; thereby, the non-radiative decay channels can be more effectively blocked to result in intense fluorescence in the mixture solutions. Molecular rotations are more effectively hampered when the An2Py molecules are located in a more crowded environment, such as in a smaller particle formed in solutions containing more hexane. Therefore, the An2Py luminogens in THF/hexane mixtures emit with higher intensity than An2Py in pure THF solvent.

Blending of An2Py with small-mass bisphenol-A (BPA)

To emphasize the role of H-bond interaction on the molecular rotation and on the emission efficiency of An2Py, different amounts of BPA were used to mix with An2Py in the solution state. Dilute solutions of An2Py/BPA(x/y) mixtures in THF were prepared under the condition that the concentration of An2Py was kept at a constant value of 10^{-5} M. As illustrated in Fig. 2A, addition of non-emissive BPA to pure An2Py causes conceivable emission intensification. The emission intensity of An2Py/BPA(1/1) solution is more than 4-fold that of the pure An2Py solution. The An2Py luminogens in the dilute solution mixtures are supposed to be locked by the BPA molecules in order to exhibit the emission enhancements. Most of the An2Py luminogens in An2Py/BPA(1/1) solution are assumed to be molecularly anchored by BPA since further increase of BPA content to An2Py/BPA(3/7) results in little emission variation,

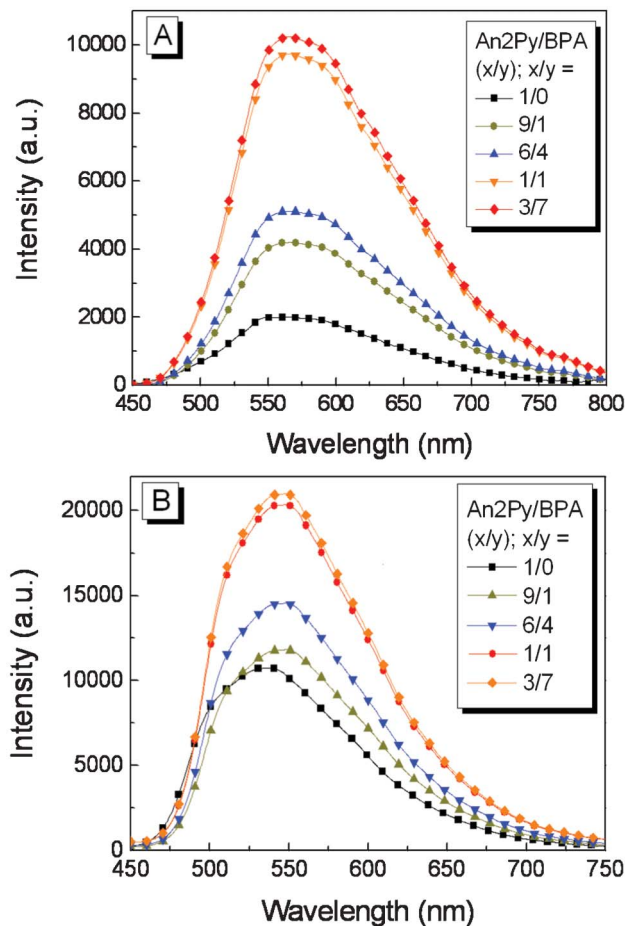


Fig. 2 The emission spectra of (A) solution (with $[\text{An2Py}] = 10^{-5} \text{ M}$) and (B) solid $\text{An2Py/BPA}(x/y)$ of different compositions (excited at 400 nm).

which indicates that H-bond interactions between An2Py and BPA proceed efficiently even in dilute solution. To verify the effectiveness of the H-bond interactions, a large excess of BPA molecules were intentionally added in separate experiments and the results suggest that overdose of BPA to a high value of 100-fold (*i.e.* $\text{An2Py/BPA} = 1/100$) gives no intensity variations compared to the $\text{An2Py/BPA}(3/7)$ solution. Under the premise that restricted molecular rotation is the key leading to enhanced emission, the amounts of BPA applied in the $\text{An2Py/BPA}(3/7)$ solution are already sufficient to impose effective restriction to result in an emission behavior similar to the $\text{An2Py/BPA}(1/100)$ solution. DLS analysis (Fig. S1A, ESI†) indicates that aggregated particles also formed in the corresponding $\text{An2Py/BPA}(x/y)$ solution mixtures and the aggregated particles progressively shrunk in size with increasing BPA content in the solution. The congestion in the shrunk nanoparticles imposes steric constraints on the molecular rotations of the An2Py luminogens; thus, An2Py molecules in the smaller particles will have stronger emission than An2Py in the larger particles due to the reduced non-radiative decay pathways.

To experimentally verify the restricted molecular rotation promoted by H-bond interactions, we carried out ^1H NMR

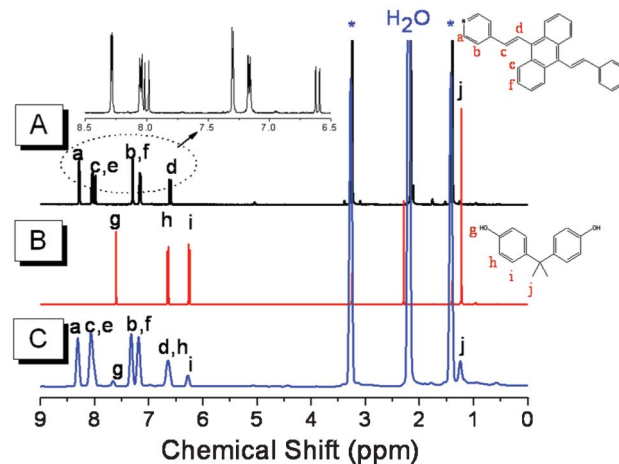


Fig. 3 Solution ^1H NMR spectra of (A) An2Py ($=10^{-5} \text{ M}$), (B) BPA ($=10^{-5} \text{ M}$) and (C) $\text{An2Py/BPA}(1/1)$ mixture (THF-d_8).

experiments on solutions of An2Py, BPA and the $\text{An2Py/BPA}(1/1)$ mixture in THF-d_8 . The ^1H NMR band shape analysis had been previously utilized to study the rotation-induced conformational changes on AIE-active organic⁴⁴ and polymeric⁴⁵ systems. In general, the fast conformational exchanges caused by the fast molecular rotations of the axes of single bonds linked to the central planar ring give sharp resonance peaks, whereas the slower exchanges due to restricted molecular rotation broaden the resonance peaks. The ^1H NMR spectra of the $\text{An2Py/BPA}(1/1)$ solution (Fig. 3C) were performed under the condition that the concentrations of An2Py and BPA were fixed at 10^{-5} M ; therefore, if there are no mutual associations between An2Py and BPA, the resonance peaks of the $\text{An2Py/BPA}(1/1)$ solution should be the same as those in the pure An2Py ($=10^{-5} \text{ M}$) (Fig. 3A) and the pure BPA ($=10^{-5} \text{ M}$) (Fig. 3B) solutions. The solution of pure An2Py in THF-d_8 exhibits the sharp, multiple resonance peaks of the aromatic (H_a , H_b , H_c and H_f) and the vinylic (H_e and H_d) protons in the range of δ 6.0 to 8.7. The sharp multiplets in the pure An2Py solution, however, became broader and indistinguishable in the spectrum of $\text{An2Py/BPA}(1/1)$ solution. The H-bond interaction forces should give the same constraint on the BPA component; therefore, the same peak broadening was observed on the aromatic (H_i) and isopropyl (H_j) proton peaks of the BPA molecules in the spectrum of $\text{An2Py/BPA}(1/1)$ solution. Suggestively, intermolecular H-bond interactions between An2Py and BPA will exert the same locking mechanism on both components and the molecular anchoring on the An2Py luminogen caused the observed enhanced emission in the mixture solutions. The ^1H NMR spectra therefore identify the existence of H-bond interactions between An2Py and BPA in the solution mixtures.

Because the molecular rotation of the AIEE-active luminogens should be more effectively restricted in the solid when compared to their solution states, we therefore expected strong fluorescence in the pure An2Py solid. Furthermore, the H-bond interactions in the solid state should be more pronounced than in the solution state due to more H-bond

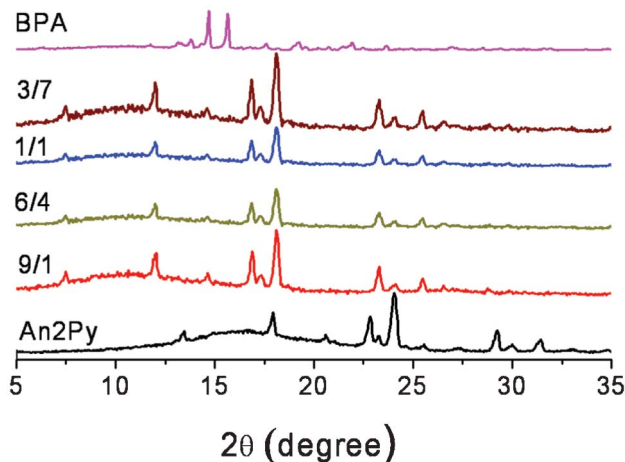


Fig. 4 Wide-angle X-ray diffraction spectra of BPA, An2Py and An2Py/BPA(*x/y*) solids of different compositions.

interaction opportunities in the closely-packed condensed solid state. To understand the solid-state fluorescence properties, preliminary characterization on the pure An2Py, BPA and the blended An2Py/BPA(*x/y*) solids was therefore conducted. Pure An2Py and BPA solids are both crystalline materials, as verified from the X-ray diffraction patterns in Fig. 4. Interestingly, all the An2Py/BPA solid blends are still crystalline materials with the resolved crystalline diffraction peaks located at positions essentially different from those in the pure An2Py and BPA components, which indicates that a new crystalline structure different from the starting An2Py and BPA forms after blending. Supposedly, this new crystalline structure should be correlated with the An2Py/BPA H-bonded species. Identical to compounds with crystalline-induced emission (CIE)⁴ behavior, the regularly-packed crystalline arrays should be the additive factor contributing to effective restriction on the molecular rotation of the luminescent An2Py in the An2Py/BPA blends. Molecular rotations of the fluorescent An2Py are considered to be largely restricted in the crystalline arrays and emission intensity of the solid blends is therefore comparatively larger than their preparative solution mixtures (compare Fig. 2A and 2B). The H-bond interactions in the solid blends can be conveniently evaluated from the FTIR analysis on the hydroxyl (3500–3100 cm⁻¹) and the pyridine (900–1000 cm⁻¹) absorption regions. The hydroxyl stretching band of the starting BPA (Fig. 5A) is discussed first: the self-associated H-bonded O–H groups contribute to the broad asymmetric absorption at 3350 cm⁻¹ and the free O–H stretching absorption should locate at 3525 cm⁻¹.^{46,47} In general, a dynamic equilibrium between free O–H and self-associated H-bonded O–H should exist in the pure BPA solid; however, the scarcity of the free O–H stretching absorption at 3525 cm⁻¹ (Fig. 5A) indicates that most O–H groups form self-associated H-bonds in the crystalline BPA solid. Upon blending with An2Py, fractions of self-associated H-bonds in BPA are broken and replaced by the intermolecular H-bonds between BPA and An2Py, which should result in the broad stretching absorption at around 3150 cm⁻¹ (*cf.* the spectra of

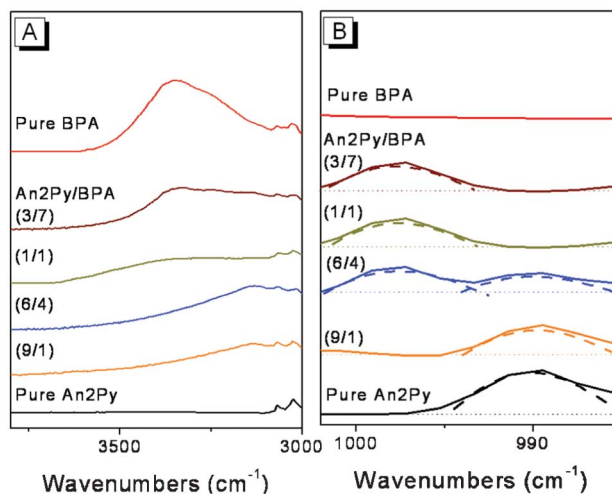


Fig. 5 Infrared spectra of solid An2Py/BPA(*x/y*) blends on (A) the hydroxyl OH and (B) the pyridine absorptions.

An2Py/BPA(9/1) in Fig. 5A). With increasing An2Py content from An2Py/BPA(3/7) to (9/1) blends, we observed the transformation of the O–H stretching bands from the predominantly self-associated (3350 cm⁻¹) to the intermolecular (3150 cm⁻¹) H-bonded OH absorptions. With excess An2Py component, An2Py/BPA(9/1) and (6/4) blends exhibit basically the intermolecular H-bonded OH absorption at 3150 cm⁻¹. The characteristic absorption band of the free pyridine ring in pure An2Py appears at 993 cm⁻¹ (Fig. 5B).⁴⁸ With the presence of BPA component, a new band due to the intermolecular H-bonded pyridine absorption emerged at around 997 cm⁻¹. It is clear that the free pyridine absorption for pure An2Py will gradually reduce in intensity. In An2Py/BPA(6/4) blend, certain pyridine rings of An2Py still remain non-bonded but in An2Py/BPA(1/1) and (3/7), most of the pyridine rings are already H-bonded to hydroxyl groups. The high fractions of H-bonded pyridine rings should contribute to the high fluorescence in An2Py/BPA(1/1) and (3/7) samples. As suggested above, the intermolecular H-bond interactions impose restriction on the An2Py luminogen and lead to enhanced emission of the blending mixtures. The influence of intermolecular H-bonds on the solid blends can be clearly demonstrated in the solid emission spectra (Fig. 2B) that the emission intensity increases with the increasing BPA content from the pure solid An2Py to the An2Py/BPA(3/7) samples. Emissions of solid samples are all higher in intensity than their respective mother solutions (*cf.* Fig. 2A), a result indicative of the effective restriction on the molecular rotations of the crystalline solid samples. The emission efficiency can be also followed by the quantum yields (Φ_F) measured from an integrating sphere; as listed in Table 1, the solid An2Py possesses a Φ_F value of 48% and with increasing BPA content in the solid, we observe the increase of Φ_F until the ultimate value of 69% was attained for An2Py/BPA(3/7) blend. Similar to the solution samples, further increase of BPA content gains no difference to the emission efficiency (*e.g.* the An2Py/BPA(1/100) and (3/7) blends have the same Φ_F value).

Table 1 Quantum yields (Φ_F)^a of the solid An2Py/BPA and An2Py/PVh blends

Solid An2Py/BPA(x/y) ^b blends						
x/y	1/0	9/1	6/4	1/1	3/7	
Φ_F (%)	48	50	57	66	69	
Solid An2Py/PVPh(x/y) ^b blends						
x/y	2/0	20/1	4/1	2/1	1/1	2/3
Φ_F (%)	48	51	54	57	66	71

^a Quantum yield, obtained from integrating sphere. ^b x/y refers to the applied molar ratio between the pyridinyl ring and the hydroxyl groups.

When the BPA content is more than 70 mol% (as in An2Py/BPA(3/7)), most of the An2Py luminogens should already be surrounded and locked by the BPA molecules through the mutual intermolecular H-bonds, further increase of the BPA (as in An2Py/BPA(1/100)) component gains no more increase of the H-bonded An2Py pairs. For a blend of An2Py/BPA(1/100), all the An2Py luminogens should be well isolated by and bonded by large amounts of BPA molecules. With less luminescent component, the solid An2Py/BPA(1/100) blend has the same emission efficiency as An2Py/BPA(3/7); therefore, effective molecular anchoring, not the content of the luminogens, is the key leading to enhanced emission in the solid blends.

An2Py to poly(vinyl phenol) (PVPh)

As similar with small-mass BPA, polymeric PVPh has the same hydroxyl functions capable of binding to An2Py with preferable H-bond interactions. Primarily, the viscous polymeric chain of the PVPh component should have more effective restriction on molecular mobility compared to small-mass BPA; however, the multiple hydroxyl pendant groups along the polymer chain of PVPh will generate lots of intermolecular physical junction points when H-bonded to BPA molecules in the solution state and the resultant crosslinked networks in the solution should prevent the hydroxyl functions from complete H-bonding. To avoid the premature precipitation of the crosslinked gels, all solution mixtures of An2Py/PVPh were agitated during the solution mixing step and the resultant solutions were sent for spectral measurement immediately after preparation (gelled masses were visible after two hours). Despite the incomplete H-bond interactions involve in the preparation step, the solution emission spectra in Fig. 6A still show the same trend that increasing PVPh content results in the increase of the emission intensity. Here, solution of An2Py/PVPh(2/3) has the highest emission intensity among all solutions and, similar to the An2Py/BPA case, further increase of PVPh content resulted in little variation of the emission intensity. It is then envisaged that H-bond interactions cannot be driven to completion in the viscous polymeric system with multiple H-bond reaction sites along the long-chain segments. The DLS analysis (Fig. S1B, ESI†) indicates that the An2Py/PVPh(x/y) solutions also contain nano-sized ($D_h = 220\text{--}140$ nm) particles and the corresponding particles shrunk in size with increasing PVPh content in the solutions. Consistent with the small-mass case,

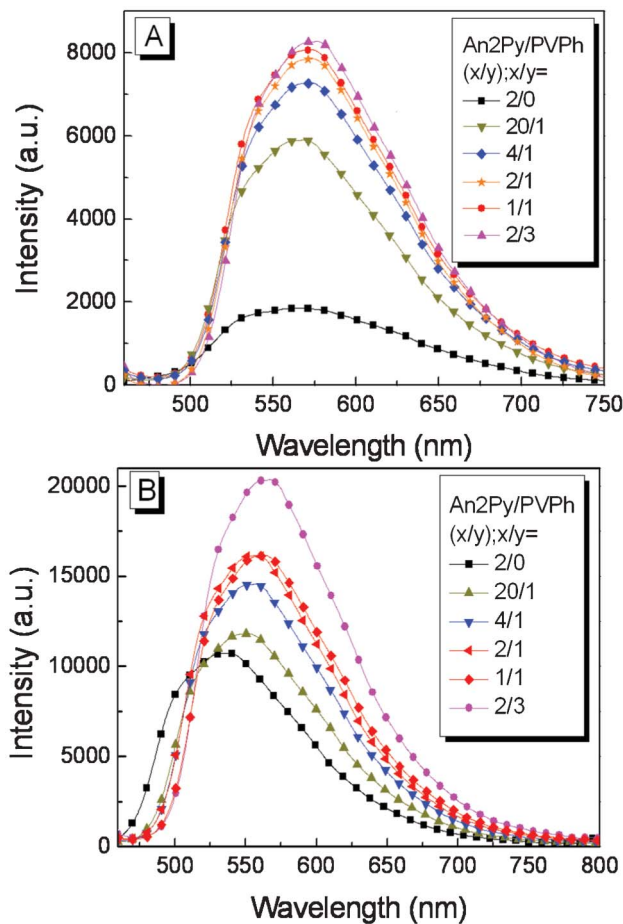


Fig. 6 The emission spectra of (A) solution An2Py/PVPh(x/y) ($[An2Py] = 10^{-5}$ M) and (B) solid An2Py/PVPh(x/y) of different compositions (excited at 400 nm).

the enhanced molecular restriction on shrunk particles also contributes to the emission intensification. The restricted molecular rotation imposed by the polymeric PVPh was also verified from the solution ¹H NMR spectra (Fig. S2, ESI†) of An2Py, PVPh and An2Py/PVPh(1/1) samples. Under the condition that the concentration of An2Py was kept at 10^{-5} M, the aromatic resonance peaks of the An2Py/PVPh(1/1) solution is comparatively broader than those in pure An2Py solution. The solid An2Py/PVPh blends from the mother solution mixtures were also inspected by WAXS. Despite the amorphous PVPh being applied in the blend, the resultant An2Py/PVPh(20/1), (4/1) and (2/1) blends have a new crystalline structure because the sharp crystalline peaks (Fig. 7) formed are at positions different from those in An2Py. With the lowest PVPh content, the An2Py/PVPh(20/1) blend has the highest crystallinity among all samples. With increasing PVPh content from An2Py/PVPh(20/1) to (2/1) blends, the crystallinity obviously decreases and no crystalline diffraction peaks are resolved in An2Py/PVPh(1/1) and (2/3) blends. The new crystal formed in An2Py/PVPh(20/1), (4/1) and (2/1) should be due to the H-bonded An2Py. Theoretically, in the An2Py/PVPh(20/1) blend, the maximum number of hydroxyl groups loaded by PVPh is only 1/20 of the pyridine rings in An2Py; therefore,

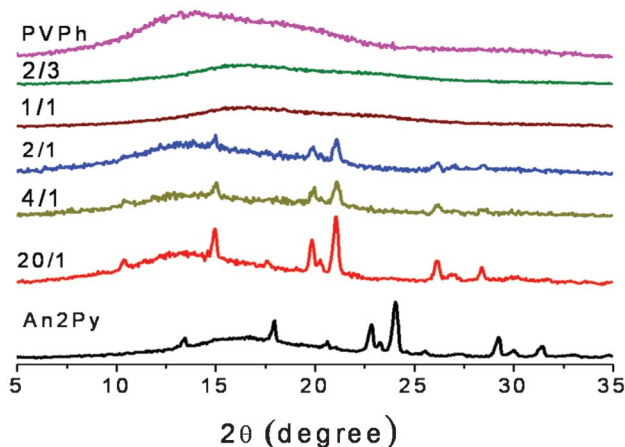


Fig. 7 Wide-angle X-ray diffraction spectra of An2Py, PVPh and An2Py/PVPh(*x/y*) blends of different compositions.

only a low fraction of An2Py molecules can be H-bonded to PVPh and cannot account for the high crystallinity resolved for An2Py/PVPh(20/1). It is possible that the small amounts of H-bonded An2Py serve as the starting crystallization loci for further deposition of non-H-bonded An2Py molecules to result in new crystals with high crystallinity. By increasing the amorphous PVPh in the blend, the regular packing of the amounts of H-bonded An2Py is reduced due to the imposed geometrical restraints from the random hydroxyl bonding sites of the amorphous crosslinked networks. In An2Py/PVPh(1/1) and (2/3) blends, the random hydroxyl bonding sites in the crosslinked networks are supposed to bind to An2Py irregularly to result in the incomplete H-bonding sites along the crosslinked networks. With increasing randomness introduced by the crosslinking network, the An2Py/PVPh(1/1) and (2/3) blends are identified to be amorphous. The resultant solid emission spectra (Fig. 6B) also exhibit the similar trend of increasing emission intensity with increasing PVPh content in the blends, which can be also confirmed by the resultant Φ_F values summarized in Table 1. A highest Φ_F value of 71% was identified for the solid An2Py/PVPh(2/3) blend and no more emission enhancement can be attained with more PVPh component loaded in the blend. The H-bond interactions are also confirmed from the corresponding infrared spectra on the hydroxyl (Fig. 8A) and the pyridine (Fig. 8B) absorption regions. Similar to An2Py/BPA system, the same transformation from the intra to the intermolecular H-bonded OH groups is resolved when the PVPh content in the blends is increased. However, in contrast to the small-mass system, certain fractions of free hydroxyl absorptions at 3525 cm^{-1} are clearly viewed as shoulder-like peaks in the spectra of An2Py/PVPh(2/1), (1/1) and (2/3) blends. The presence of free hydroxyl groups in blends of high PVPh content is consistent with the above-mentioned concept that complete intermolecular H-bond interactions are difficult to attain in the crosslinking system. Pyridine absorptions (Fig. 8B) in the range of $985\text{ to }1020\text{ cm}^{-1}$ were subjected to curve-fitting to have a clear view of the bonding situation on the pyridine ring. Here, the phenol absorption⁴⁹ at 1012 cm^{-1} should be separated from the

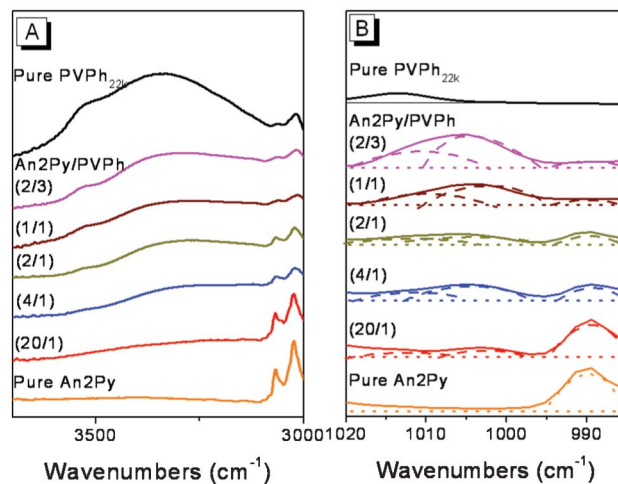


Fig. 8 Solid infrared spectra of An2Py/PVPh(*x/y*) blends on (A) the hydroxyl OH and (B) the pyridine absorptions.

bonded pyridine absorption at 1005 cm^{-1} . As indicated by the deconvoluted results (dashed curves) shown in Fig. 8B, the free pyridine absorptions at 993 cm^{-1} decrease their contribution with increasing PVPh content in the blends. Nevertheless, even with the large amounts of PVPh, the An2Py/PVPh(2/3) blend still contains a certain amount of residual pyridine rings remaining non-bonded, which is consistent with the observed free OH absorption at 3525 cm^{-1} .

Qualitative comparisons of the An2Py/BPA, An2Py/PVPh and the previous PFN/PVR systems

The qualitative comparison on the small-mass BPA and the polymeric PVPh as molecular anchors to restrict rotation of the An2Py are illustrated here. For An2Py/PVPh system, the viscous chain segments in the physically crosslinked networks are primarily considered to have efficient restriction forces on the molecular rotation. Nevertheless, the geometrical constraints on the highly-crosslinked samples also prohibit complete H-bond interactions and result in less H-bonded pairs to provide fluorescence with enhanced efficiency. On the other hand, the mobile small-mass BPA generates no viscous, physical-crosslinked product as PVPh does but the thorough H-bond interactions in the highly-crystalline blended products furnish effective restriction on molecular rotation and result in fluorescence with intensity comparable to the polymeric An2Py/PVPh system. The ultimate emission efficiencies (69 vs. 71%) attained for both An2Py/BPA and An2Py/PVPh are therefore comparable. Our initiative for the present study was aimed at the high molecular mobility of the small-mass An2Py, which should furnish high contact possibility with other H-bond donors to result in a high number of H-bonded pairs in the preparative solution and therefore the solid blend states. However, the ultimate emission yields (69 and 71%) obtained in this study are comparatively lower than those (93%) from the PFN/PVR blends.⁴¹ The pure rigid-chain PFN solid already has a high quantum yield of 61% and an increase of PVR content in the PFN/PVR blends raised the quantum efficiency to an ultimate value of 93% for the PFN/PVR(1/200)

blend. Instead of molecular mobility to create a high number of H-bond pairs, the preliminary structural factor of chain rigidity seems to be more crucial for deciding the final emission performances of the blend systems. The molecular rotations of the luminogenic units in PFN polymer were supposed to be effectively hampered by the rigid main-chain framework and addition of PVR continuously introduced rotational constraints by H-bond interactions and resulted in the ultimate quantum efficiency of 93% for PFN/PVE(1/200) with small amounts (~2.3 wt%) of fluorescent PFN component. For the present system, the molecular mobility of the mobile An2Py can be frozen by H-bond interaction, too; however, to a lesser extent compared to the rigid PFN system due to the mobile nature of the small-mass An2Py. Therefore, molecular rotation of the rigid main-chain polymeric luminogens are said to be more efficiently restricted by H-bond interactions compared to the small-mass organic luminogens.

Conclusion

An2Py with two pyridine terminal rings was successfully prepared by a Heck coupling reaction and was used to H-bond with small-mass BPA and the polymeric PVPh, respectively, to construct fluorescence systems with enhanced emissions. Primarily, An2Py was proven to be AIEE-active according to the emission behavior in the THF/hexane solvent/poor solvent mixtures. With increasing content of H-bond donors (*i.e.* BPA and PVPh), both An2Py/BPA and An2Py/PVPh systems show enhanced emissions in the solution and in the solid states. Results from the solution ¹H NMR spectra suggest that molecular rotations of the An2Py luminogens are hampered by H-bond interactions. Solution and solid blends of An2Py/BPA(3/7) and An2Py/PVPh(2/3) possess the highest emission efficiencies and no more intensity gain is observed when more H-bond donors were loaded. Polymer PVPh provides the beneficial viscous chain to impose effective molecular restriction on the An2Py luminogens; however, the incomplete H-bond interactions in the highly-crosslinked products give less H-bond pairs and less emission enhancements. On the other hand, the thorough H-bond interactions and the highly-crystalline structures in the An2Py/BPA blends furnish effective restriction on molecular rotation and result in fluorescence with intensity comparable to the polymeric An2Py/PVPh system. The ultimate emission efficiencies (69 vs. 71%) are therefore quite close for both systems.

Acknowledgements

We appreciate the financial support from National Science Council, Taiwan under the contract no. 101-2221-E-110-022.

References

- J. Luo, Z. Xie, J. W. Y. Lam, L. Cheng, H. Chen, C. Qiu, H. S. Kwok, X. Zhan, Y. Liu, D. Zhu and B. Z. Tang, *Chem. Commun.*, 2001, 1740.
- B. Z. Tang, X. Zhan, G. Yu, P. P. S. Lee, Y. Liu and D. Zhu, *J. Mater. Chem.*, 2001, **11**, 2974.
- J. Wu, W. Liu, J. Ge, H. Zhang and P. Wang, *Chem. Soc. Rev.*, 2011, **40**, 3483.
- Y. Hong, J. W. Y. Lam and B. Z. Tang, *Chem. Commun.*, 2009, 4332.
- J. Liu, J. W. Y. Lam and B. Z. Tang, *J. Inorg. Organomet. Polym. Mater.*, 2009, **19**, 249.
- A. Qin, J. W. Y. Lam and B. Z. Tang, *Prog. Polym. Sci.*, 2012, **37**, 182.
- C. J. Bhongale and C. S. Hsu, *Angew. Chem., Int. Ed.*, 2006, **45**, 1404.
- S. Dong, Z. Li and J. Qin, *J. Phys. Chem. B*, 2009, **113**, 434.
- B. K. An, S. K. Kwon, S. D. Jung and S. Y. Park, *J. Am. Chem. Soc.*, 2002, **124**, 14410.
- Z. Wang, H. Shao, J. Ye, L. Tang and P. Lu, *J. Phys. Chem. B*, 2005, **109**, 19627.
- C. X. Yuan, X. T. Tao, L. Wang, J. X. Yang and M. H. Jiang, *J. Phys. Chem. C*, 2009, **113**, 6809.
- Z. Yang, Z. Chi, T. Yu, X. Zhang, M. Chen, B. Xu, S. Liu, Y. Zhang and J. Xu, *J. Mater. Chem.*, 2009, **19**, 5541.
- W. Z. Yuan, P. Lu, S. Chen, J. W. Y. Lam, Z. Wang, Y. Liu, H. S. Kwok, Y. Ma and B. Z. Tang, *Adv. Mater.*, 2010, **22**, 2159.
- B. Xu, Z. Chi, Z. Yang, J. Chen, S. Deng, H. Li, X. Li, Y. Zhang, N. Xu and J. Xu, *J. Mater. Chem.*, 2010, **20**, 4135.
- Z. Zhao, S. Chen, J. W. Y. Lam, C. K. W. Jim, C. Y. K. Chan, Z. Wang, P. Lu, C. Deng, H. S. Kwok, Y. Ma and B. Z. Tang, *J. Phys. Chem. C*, 2010, **114**, 7963.
- W. Wang, T. Lin, M. Wang, T. X. Liu, L. Ren, D. Chen and S. Huang, *J. Phys. Chem. B*, 2010, **114**, 5983.
- K. Kokado and Y. Chujo, *Macromolecules*, 2009, **42**, 1418.
- A. Pucci, R. Rausa and F. Ciardelli, *Macromol. Chem. Phys.*, 2008, **209**, 900.
- J. Liu, Y. Zhong, J. W. Y. Lam, P. Lu, Y. Hong, Y. Yu, Y. Yue, M. Faisal, H. H. Y. Sung, I. D. Williams, K. S. Wong and B. Z. Tang, *Macromolecules*, 2010, **43**, 4921.
- C. T. Lai and J. L. Hong, *J. Phys. Chem. B*, 2010, **114**, 10302.
- C. A. Chou, R. H. Chien, C. T. Lai and J. L. Hong, *Chem. Phys. Lett.*, 2010, **501**, 80.
- T. Liu, X. Tao, F. Wang, X. Dang, D. Zou, Y. Ren and M. Jiang, *J. Phys. Chem. C*, 2008, **112**, 3975.
- P. Chen, R. Lu, P. Xue, T. Xu, G. Chen and Y. Zhao, *Langmuir*, 2009, **25**, 8395.
- F. Camerel, L. Bonardi, M. Schmutz and R. Ziessel, *J. Am. Chem. Soc.*, 2006, **128**, 4548.
- P. Zhang, H. Wang, H. Liu and M. Li, *Langmuir*, 2010, **26**, 10183.
- H. H. Fang, Q. D. Chen, J. Yang, H. Xia, B. R. Gao, J. Feng, Y. G. Ma and H. B. Sun, *J. Phys. Chem. C*, 2010, **114**, 11958.
- Z. Yang, Z. Chi, B. Xu, H. Li, X. Zhang, X. Li, S. Liu, Y. Zhang and J. Xu, *J. Mater. Chem.*, 2010, **20**, 7352.
- C. T. Lai and J. L. Hong, *J. Mater. Chem.*, 2012, **22**, 9546.
- H. Li, Z. Chi, B. Xu, X. Zhang, Z. Yang, X. Li, S. Liu, Y. Zhang and J. Xu, *J. Mater. Chem.*, 2010, **20**, 6103.
- S. Dong, Z. Li and J. Qin, *J. Phys. Chem. B*, 2009, **113**, 434.
- Q. Zeng, Z. Li, Y. Dong, C. Di, A. Qin, Y. Hong, L. Ji, Z. Zhu, C. Jim and G. Yu, *Chem. Commun.*, 2007, 70.
- J. Chen, C. C. W. Law, J. W. Y. Lam, Y. Dong, S. M. F. Lo, I. D. Williams, D. Zhu and B. Z. Tang, *Chem. Mater.*, 2003, **15**, 1535.

- 33 Z. Li, Y. Dong, B. Mi, Y. Tang, M. Haüssler, H. Tong, Y. Dong, J. W. Y. Lam, Y. Ren, H. H. Y. Sung, K. S. Wong, P. Gao, I. D. Williams, H. S. Kwok and B. Z. Tang, *J. Phys. Chem. B*, 2005, **109**, 10061.
- 34 Y. Liu, X. Tao, F. Wang, J. Shi, J. Sun, W. Yu, Y. Ren, D. Zou and M. Jiang, *J. Phys. Chem. C*, 2007, **111**, 6544.
- 35 P. Chen, R. Lu, P. Xue, T. Xu, G. Chen and Y. Zhao, *Langmuir*, 2009, **25**, 8395.
- 36 P. Zhang, H. Wang, H. Liu and M. Li, *Langmuir*, 2010, **26**, 10183.
- 37 T. H. Kim, M. S. Choi, B. H. Sohn, S. Y. Park, W. S. Lyoo and T. S. Lee, *Chem. Commun.*, 2008, 2364.
- 38 J. H. Wan, L. Y. Mao, Y. B. Li, Z. F. Li, H. Y. Qiu, C. Wang and G. Q. Lai, *Soft Matter*, 2010, **6**, 3195.
- 39 M. K. Nayak, *J. Photochem. Photobiol., A*, 2011, **217**, 40.
- 40 R. H. Chien, C. T. Lai and J. L. Hong, *J. Phys. Chem. C*, 2011, **115**, 12358.
- 41 R. H. Chien, C. T. Lai and J. L. Hong, *J. Phys. Chem. C*, 2011, **115**, 20732.
- 42 D. Stern, N. Finkelmeier and D. Stalke, *Chem. Commun.*, 2011, **47**, 2113.
- 43 J. He, B. Xu, F. Chen, H. Xia, K. Li, L. Ye and W. J. Tian, *J. Phys. Chem. C*, 2009, **113**, 9892.
- 44 J. Chen, C. C. W. Law, J. W. Y. Lam, Y. Dong, S. M. F. Lo, I. D. Williams, D. Zhu and B. Z. Tang, *Chem. Mater.*, 2003, **15**, 1535.
- 45 C. T. Lai and J. L. Hong, *J. Mater. Chem.*, 2012, **22**, 9546.
- 46 B. Fei, C. Chen, S. Peng, X. Zhao, X. Wang and L. Dong, *Polym. Int.*, 2004, **53**, 2092.
- 47 W. C. Chen, S. W. Kuo, U. S. Jeng and F. C. Chang, *Macromolecules*, 2008, **41**, 1401.
- 48 C. H. Lu, S. W. Kuo, W. T. Chang and F. C. Chang, *Macromol. Rapid Commun.*, 2009, **30**, 2121.
- 49 W. C. Chen, S. W. Kuo, U. S. Jeng and F. C. Chang, *Macromolecules*, 2009, **42**, 3580.